MOLECULAR AND CELLULAR BIOLOGY, July 2006, p. 5373–5381 Vol. 26, No. 14
0270-7306/06/$08.00+0 doi:10.1128/MCB.00043-06

Mouse *emi1* Has an Essential Function in Mitotic Progression during Early Embryogenesis†

Ho Lee,[1,2] Dong Jun Lee,[1] Sang Phil Oh,[1] Hee Dong Park,[1] Hyun Hee Nam,[3] Jin Man Kim,[3] and Dae-Sik Lim[1]*

Department of Biological Sciences and Biomedical Research Center, Korea Advanced Institute of Science and Technology, 373-1 Guseoung-dong, Yuseong-gu, Daejeon 305-701, South Korea[1]; National Cancer Center, 809 Madu1-dong, Ilsandon-gu, Goyang-si, Gyeonggi-do 410-769, South Korea[2]; and Department of Pathology, College of Medicine, Chungnam National University, 6 Munwha-dong Jung-gu, Daejeon 301-131, South Korea[3]

Received 9 January 2006/Returned for modification 2 February 2006/Accepted 28 April 2006

For successful mitotic entry and spindle assembly, mitosis-promoting factors are activated at the G_2/M transition stage, followed by stimulation of the anaphase-promoting complex (APC), an E3 ubiquitin ligase, to direct the ordered destruction of several critical mitotic regulators. Given that inhibition of APC activity is important for preventing premature or improper ubiquitination and destruction of substrates, several modulators and their regulation mechanisms have been studied. Emi1, an early mitotic inhibitor, is one of these regulatory factors. Here we show, by analyzing Emi1-deficient embryos, that Emi1 is essential for precise mitotic progression during early embryogenesis. Emi1$^{-/-}$ embryos were found to be lethal due to a defect in preimplantation development. Cell proliferation appeared to be normal, but mitotic progression was severely defective during embryonic cleavage. Moreover, multipolar spindles and misaligned chromosomes were frequently observed in Emi1 mutant cells, possibly due to premature APC activation. Our results collectively suggest that the late prophase checkpoint function of Emi1 is essential for accurate mitotic progression and embryonic viability.

To successfully enter mitosis and assemble the mitotic spindle, cells undergo a series of timed and interdependent regulatory events. The activation of mitosis-promoting factor (MPF), a complex of cyclin B and Cdk1, orchestrates a series of structural and regulatory events via phosphorylation of key mitotic substrates (21). Next, the anaphase-promoting complex (APC), an E3 ubiquitin ligase that controls the ubiquitin-dependent destruction of mitotic cyclins, is activated to direct the ordered impairment of several critical regulators, including the early mitotic regulator cyclin A at late prophase, the chromosome cohesion regulator securin at metaphase, and cyclin B in late mitosis (2, 9, 24).

APC activity is temporally regulated through binding of the complex with either of two activating subunits, Cdc20 or Cdh1 (2, 9). Cdc20 activates APC during early mitosis until anaphase, whereas Cdh1 functions during late mitosis and the G_1 phase. APC-Cdc20 activity is regulated via three types of inhibitory proteins or complexes that antagonize Cdc20 function: (i) components of the spindle assembly checkpoint, including at least seven proteins (Bub1, Bub2, Bub3, Mad1, Mad2, Mad3 [BubR1], and Mps1) (16, 22, 40), (ii) the early mitotic inhibitor Emi1 (27, 28), and (iii) the Ras association domain family 1A (Rassf1A) (31, 32). Emi2/Erp1/FBXO43, the Emi1-related protein 1, has recently been reported as another APC-Cdc20 inhibitor during cytostatic factor (CSF) arrest whose inhibitory mechanism remains to be further analyzed (30, 34).

To determine the physiological functions of these APC inhibitors, genetic analyses in mice were performed. The spindle checkpoint proteins Mad2, BubR1, and Bub3 were found to be essential for early development in gene-disrupted mice, as evident from their failure to survive between days 6.5 and 8.5 postcoitus due to extensive apoptosis (4, 14, 37). Null embryos treated with a spindle depolymerization agent failed to arrest in metaphase and displayed increased mitotic abnormalities. Mad2 haploinsufficiency causes premature anaphase and chromosome instability (19), while BubR1 haploinsufficiency induces an increase in the number of splenic megakaryocytes, resulting from spindle checkpoint failure (37). These results confirm that the spindle assembly checkpoint is essential for accurate chromosome segregation in mitotic mouse cells and embryonic viability. *rassf1A*-targeted mice were viable and fertile but prone to spontaneous tumorigenesis at an advanced age (18 to 20 months) (33, 36). Tumors in *rassf1A*-targeted mice included lung adenomas, lymphomas, and breast adenocarcinoma. Genetic analyses for Emi1 and Emi2 in mice have not been reported until now. Our present study on *emi1*-targeted mice is the first account of the physiological importance of Emi1.

Emi1 was initially identified in *Drosophila* as a gene product, rca1 (regulator of cyclin A), that induces cyclin A accumulation (5). Emi1 inhibits APC-Cdc20 activity at interphase in the *Xenopus* embryo by blocking binding of the Cdc20 adaptor to its substrates, thus preventing mitotic cyclin destruction (27, 28). The protein additionally regulates the APC-Cdh1 complex in somatic cells to induce the stabilization of S-phase regulators, including cyclin A, at G_1-S transition (12). Specifically,

* Corresponding author. Mailing address: Department of Biological Sciences, Biomedical Research Center, Korea Advanced Institute of Science and Technology, 373-1 Guseoung-dong, Yuseong-gu, Daejeon 305-701, South Korea. Phone: 82-42-869-2635. Fax: 82-42-869-2610. E-mail: daesiklim@kaist.ac.kr.

† Supplemental material for this article may be found at http://mcb.asm.org/.

Emi1 ensures an interval of cyclin stability from late G_1 phase to early mitosis by inhibiting APC-Cdh1 and Cdc20 activity. At the beginning of this interval, Emi1 is upregulated by the E2F transcription factor. At the end, Emi1 is ubiquitinated and destroyed close to the time of cyclin A impairment (12, 18).

Emi1 destruction in early mitosis, mediated by $SCF^{\beta TrCP}$ ubiquitin ligase, is required for APC activation (7, 18). The failure of βTrCP-dependent Emi1 destruction stabilizes APC substrates and results in a mitotic catastrophe, including centrosome overduplication. On the basis of these findings, it has been proposed that Emi1 destruction relieves a late prophase checkpoint for APC activation. βTrCP, a substrate-adapting subunit of the SCF complex, specifically recognizes a canonical DSGXXS motif within IκB, β-catenin, Emi1, and other substrates when both serine residues are phosphorylated (1, 6, 10, 18, 38). Mitotic phosphorylation of the Emi1 DSGxxS motif is mediated by MPF and Polo-like kinase 1 (8, 18, 20). Since $SCF^{\beta TrCP}$ is constitutively active, the timing of Emi1 destruction must be strongly governed by its phosphorylation.

Emi2/XErp1/FBXO43, a homolog of Emi1, has recently emerged as the most likely candidate to inhibit the APC during CSF arrest in *Xenopus* eggs (30, 34). Emi2 is destroyed in a process similar to the destruction pathway for Emi1. However, the APC-inhibitory role of the protein in other vertebrates is not yet reported. Also, the physiological function of Emi1 and Emi2 and their functional redundancies remain to be clarified in the whole-mouse system.

To further determine the in vivo function of Emi1, we performed genetic disruption in mice using gene-targeting techniques. We found that Emi1-knockout embryos die at the preimplantation stage and show defects in mitotic progression, chromosomal missegregation, and increased apoptosis. Based on the data obtained, we propose that the late prophase checkpoint function of Emi1 is essential for mitotic fidelity during early embryogenesis.

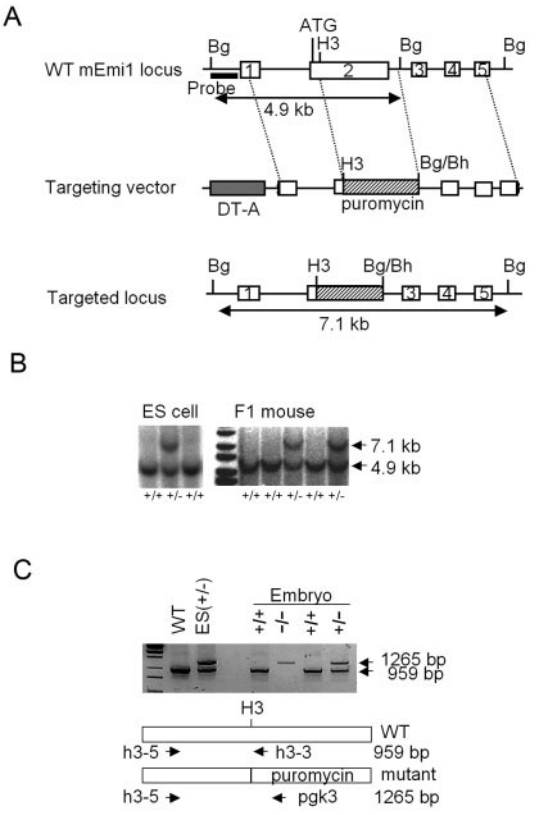

FIG. 1. Targeting strategy of the Emi1 locus. (A) Structures of the mouse Emi1 locus, targeting vector, and targeted allele after homologous recombination. Open boxes denote exons. The pgk-puromycin resistance cassette (hatched box) replaces Emi1 exon 2. The gray box represents a polymerase II promoter-diphtheria toxin A chain (DT-A) used for negative selection of ES cells. Only restriction sites relevant to the targeting construct and screening strategies are specified. Bg, BglII; H3, HindIII; Bh, BamHI. (B) Southern blot analyses of representative $Emi1^{+/-}$ ES cell clones and mice. Homologous recombination was verified using external digests and 5′ external probes. For BglII digestion, the bands representing WT and mutant alleles are 4.9 kb and 7.1 kb, respectively. The genomic position employed as a probe is shown in panel A. Left panel, confirmation of Emi1 disruption in ES cell clones. Right panel, confirmation of germ line transmission of the disrupted Emi1 allele in mice. (C) Genotyping of preimplantation embryos by PCR analysis. Recovered or in vitro-cultured embryos were genotyped by PCR using the specified primers. Separate reactions were performed to amplify the WT Emi1 allele (959 bp) and the disrupted allele (1,265 bp), and samples were combined and analyzed on ethidium bromide-stained agarose gels. H3, HindIII.

MATERIALS AND METHODS

Emi1 gene-targeting vector. The Emi1 knockout vector was generated by high-fidelity PCR with proofreading *Pfu* turbo DNA polymerase (Stratagene) and 129/Sv mouse embryonic stem (ES) cell genomic DNA as the template. Primers for the left and right arms include L5(XbaI), 5′-CCTT*TCTAGA*GCTG CGGCTCGGCGCCT-3′, and R3(SalI), 5′-GGCA*GTCGAC*CCACTTTACAG CTGGCTTTTAG-3′, respectively. Underlined letters indicate XbaI and SalI sites. The 5,812-bp PCR product was cloned in the XbaI-SalI site of pBluescript(+) KS and verified by sequencing. A phosphoglycerokinase (pgk)-puromycin poly(A) resistance cassette was inserted within the HindIII-BglII site, leading to disruption of exon 2 of mouse Emi1. The diphtheria toxin A chain cassette was employed as a negative selection marker.

Mouse ES cells were maintained on a monolayer of puromycin-resistant SNL6 feeders (17) and cultured in conditioned ES medium composed of Dulbecco's modified Eagle's medium (WelGENE, Inc., South Korea) supplemented with leukemia inhibitory factor (1,000 U/ml; Chemicon), 15% heat-inactivated fetal bovine serum (HyClone), 2 mM L-glutamine (GIBCO BRL), 0.1 mM nonessential amino acid solution (GIBCO BRL), penicillin G (100 U/ml), streptomycin sulfate (100 μg/ml), and 50 μM β-mercaptoethanol (GIBCO BRL).

The Emi1-targeting vector was linearized with KpnI and introduced into ES cells by electroporation using a gene pulser (1 pulse of 0.23 kV and 500 μF; Bio-Rad). Resistant ES cell clones grown in conditioned medium were isolated after an 8-day culture. Homologous recombination was confirmed by Southern blot analysis of genomic DNA prepared from puromycin-resistant ES cell clones using external probes, as indicated in Fig. 1B. The 5′ external probe (803 bp) was obtained by PCR using two primers, Pr5, 5′-AAGTTAGGCCGCGCCCTCAG-3′, and Pr3, 5′-AGGCGCCGAGCCGCAGCTCT-3′ (Fig. 1A). In all colonies with an apparent knockout allele, correct targeting was verified using an internal hybridization probe (a 936-bp BamHI-BglII fragment containing exons 4 and 5) (data not shown).

Two of the several correctly targeted $Emi1^{+/-}$ ES cell clones (confirmed as carrying a single-copy integration at the Emi1 locus) were subsequently injected into C57BL/6 blastocysts, resulting in germ line-transmitting chimeric mice.

In vitro culture and genotyping of preimplantation embryos. All embryos were generated by natural mating of Emi1 heterozygote animals. The morning of the day on which a vaginal plug was detected was designated day E0.5. Embryos were collected on E0.5 or E3.5 by tearing the ampulla of oviduct or flushing uteri with M2 medium (Sigma), followed by culturing in M16 medium (Sigma) for the appropriate times (23).

For genotyping, individual embryos were lysed by incubation at 55°C overnight in 5 μl PCR lysis buffer (10 mM Tris-Cl, pH 8.0, 50 mM KCl, 2 mM $MgCl_2$, 0.45% NP-40, 0.45% Tween 20, 0.2 mg/ml of proteinase K) (15). To detect the wild-type (WT) and mutant Emi1 alleles, amplification reactions were performed (as for Fig. 1C) with the following primers: h3-5 (5′-GGAGTATGGAATTCC

TTAATCTGC-3′), h3-3 (5-TCCAAACACACGGGACTGTA), and pgk-3 (5′-GCACGAGACTAGTGAGACGTGCTAC-3′). The amplification protocol included an initial incubation step at 94°C for 5 min, followed by 35 cycles of 30 s of denaturation at 94°C, 30 s of annealing at 55°C, and 50 s of elongation at 72°C with *Taq* polymerase. WT and mutant alleles yielded products of 959 bp and 1,265 bp, respectively.

Immunocytochemistry. In vitro-cultured embryos were washed twice in phosphate-buffered saline (PBS), fixed in 4% paraformaldehyde in PBS for 30 min at 4°C, and permeabilized for 20 min at room temperature in PBS containing 0.3% Triton X-100 and 1.0% bovine serum albumin. For 5-bromo-2-deoxyuridine (BrdU)-treated embryos, DNA was denatured after permeabilization with 2 N HCl-0.5% Triton X-100 for 20 min at room temperature and washed extensively in PBS with 1.0% bovine serum albumin. Embryos were incubated with specific primary antibodies overnight at 4°C. The primary antibodies used in this study were mouse anti-BrdU (Developmental Studies Hybridoma Bank), rabbit anti-phosphohistone H3 (Ser-10) (Cell Signaling Technology), mouse anti-α-tubulin, rabbit anti-cyclin A, and mouse anti-cyclin D1 (Santa Cruz Biotechnology). Incubation with fluorescein isothiocyanate or rhodamine-conjugated secondary antibodies (Santa Cruz Biotechnology) and DAPI (4′,6′-diamidino-2-phenylindole) was performed for 1 h at 37°C.

In situ hybridization. A 489-bp HindIII/SacI mouse Emi1 cDNA fragment was cloned in pBluescriptII KS(+) (Clonetech) and employed to generate riboprobes using a digoxigenin RNA-labeling kit (Roche Applied Science). Paraffin sections (4 μm) were mounted on slides coated with 3-aminopropyltriethoxy silane (Sigma) and fixed in 4% paraformaldehyde solution in PBS. In situ hybridization was performed as described previously (39).

RESULTS

Disruption of the murine *emi1* gene. The human and murine *emi1* genes, located on chromosomes 6q25 and 10A1, respectively, share a highly conserved genomic organization composed of five exons distributed over about 6 kb (Fig. 1A). Mouse genomic *emi1* was compared with its cDNA, and the exon-intron structure was determined. In our gene targeting strategy, exon 2 of murine *emi1* (encoding amino acids 1 to 210 of the Emi1 protein) was replaced with a puromycin cassette (Fig. 1A). Consequently, only the first 16 of the 383 amino acids of Emi1 were correctly translated following gene disruption with the selection cassette.

The Emi1-targeting construct was electroporated into AK7 (129/Sv) ES cells, and puromycin-resistant clones were screened for homologous recombination by Southern blotting with 5′ external probes and BglII digestion, as specified in Fig. 1B. Out of the 192 puromycin-resistant cell lines, 6 (3.1%) displayed the desired target. Mice containing the above-mentioned *emi1* mutation were generated with two targeted clones. Both clones were transmitted through germ line after crossing chimeric mice with C57BL/6 females (Fig. 1B).

Emi1 is essential for preimplantation embryo development. Heterozygous Emi1$^{+/-}$ mice were apparently normal, healthy, and fertile with no developmental abnormalities detectable over an 18-month observation period (data not shown). In contrast, no homozygous Emi1-deficient animals were produced out of 185 live births from Emi1$^{+/-}$ intercrosses (Table 1), indicating that one functional *emi1* allele is sufficient to support full embryonic and tissue development, whereas inactivation of both alleles leads to embryonic lethality.

To assess the specific period of Emi1 knockout developmental failure, timed heterozygous mating was performed. Embryos were collected at different times of gestation and genotyped by PCR. No homozygous mutant embryos were recovered at E7.5 or beyond, and completely resorbed embryos were frequent at E6.5 and E7.5 (Fig. 2B). Blastocysts at E3.5 were recovered from heterozygote intercrosses. Emi1 homozygous mutants were morphologically distinguishable from WT and heterozygous embryos in that they showed abnormal morphologie (Fig. 2A). These data indicate that Emi1-deficient embryos die at the preimplantation stage (Table 1).

TABLE 1. Genotypes of progeny from Emi1-heterozygous intercrosses[a]

Age (dpc)/parameter	No. (%) of mice with indicated genotype			No. (%) resorbed embryos	Total
	+/+	+/−	−/−		
Neonates	64 (35)	121 (65)	0 (0)		185
E9.5	12 (29)	26 (62)	0 (0)	4 (9)	42
E7.5	8 (32)	12 (48)	0 (0)	5 (20)	25
E3.5	16 (25)	36 (57)	11 (18)	NA	63
E0.5[b]	18 (18)	48 (49)	32 (33)	NA	98
Blastocyst outgrowth[c]	17 (32)	27 (52)	2 (4)	6 (12)[d]	52

[a] dpc, days postcoitum; NA, not applicable.
[b] Results show genotyping after in vitro culture of pronuclei.
[c] Results show genotyping after blastocyst outgrowth.
[d] No growth.

To further define the defects in preimplantation development of Emi1-null embryos, pronuclei were recovered from heterozygote intercrosses at swollen ampullae of oviducts and grown in vitro (23). After a 4-day culture, embryos were divided in three categories according to appearance. Specifically, 43% of pronuclei developed in normal blastocysts, 28% in morulas, and 29% in abnormal blastocysts (Fig. 2C). Genotyping by PCR revealed that most type I and II embryos were either WT or heterozygotes, whereas all type III embryos were Emi1 null.

To assess the time of preimplantation developmental failure, we analyzed embryos at different periods of in vitro culture (Fig. 2D). Pronuclei underwent continual cell division with no embryo growth and developed into blastocysts. WT and heterozygote embryos normally developed into blastocysts after 120 h culture, as confirmed by the formation of distinct inner cell mass (ICM), blastocoel cavity, and trophoblasts. Emi1-deficient embryos displayed normal development until the four-cell stage. However, Emi1-deficient embryos at 8- to 16-cell stages appeared to be abnormal and eventually developed into abnormal blastocysts. Most Emi1-null embryos displayed gross cellular degeneration and absence of distinct inner cell mass, blastocoel, or trophoblast. Accordingly, we conclude that Emi1-deficient embryos are defective in preimplantation development.

To further characterize the growth defects of Emi1-null embryos, blastocysts recovered 3.5 days later from heterozygote intercrosses were cultured in vitro for several days (23). After a 5-day culture, spherical blastocysts flatten onto the culture dish and form a multicomponent structure in which the inner cell mass grows as a round shape on top of the extraembryonic trophoblast giant (TG) cells (Fig. 2E). In these cultures, Emi1 heterozygous and WT embryonic cells normally develop into ICM and TG cells. However, only 2 out of 46 cultured embryos were Emi1-null embryos (Table 1) and their ICM displayed severely retarded outgrowth, and very few Emi1$^{-/-}$ ICM cells persisted to day 5. Phase-contrast microscopy revealed similar numbers of TG cells in mutant and control-attached embryos.

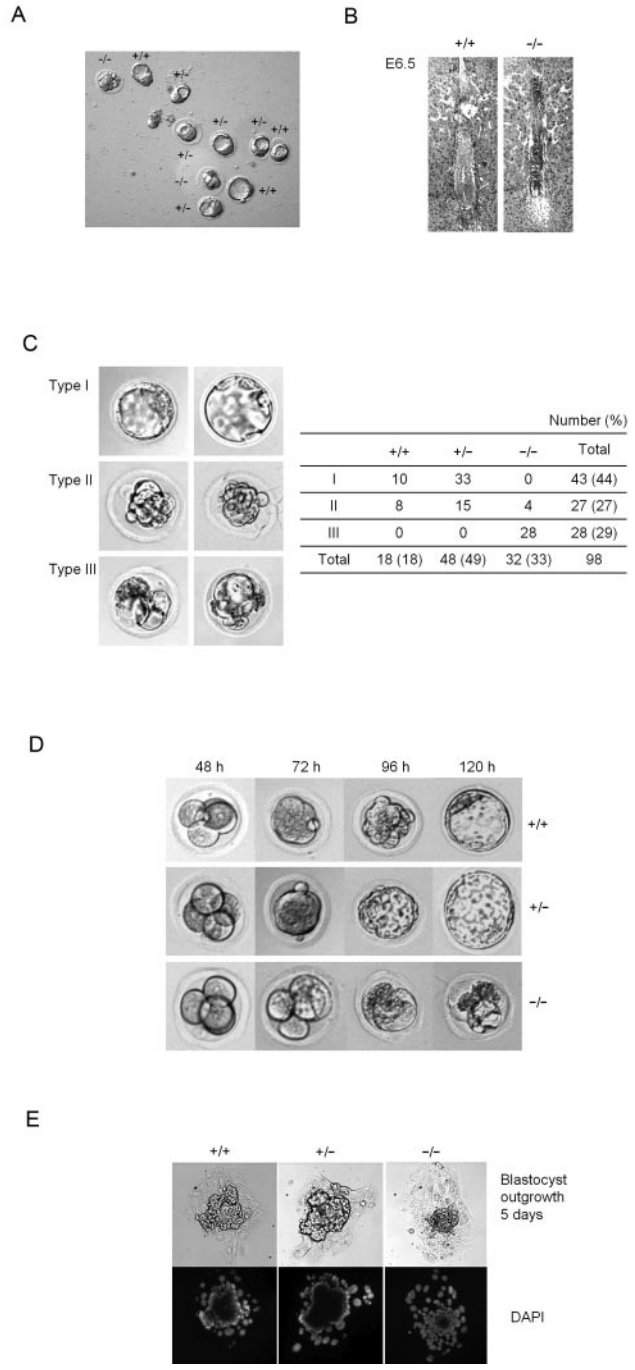

FIG. 2. Emi1 disruption results in early embryonic lethality. (A) Images of embryos at E3.5 were obtained under bright-field conditions, and the genotypes of the embryos are indicated. The Emi1$^{-/-}$ embryos appeared morphologically abnormal. (B) Hematoxylin and eosin staining of histologic sections was employed to analyze the appearance of E6.5 embryos developing in the uterus. Typical pictures of WT and fully resorbed Emi1$^{-/-}$ embryos are displayed in the left and right panels, respectively. (C) Preimplantation development of Emi1-deficient embryos. Pronuclei recovered from heterozygous intercrosses were cultured in vitro for 96 h and genotyped. Embryos were divided into three categories by appearance, specifically, type I, normal blastocysts; type II, morulas; and type III, abnormal blastocysts. (D) Time-lapsed picture of each embryo during preimplantation development. The numbers specify in vitro culture time. (E) Impaired in vitro development of Emi1-deficient embryos. Blastocyst stage embryos recovered 3.5 days later from heterozygote intercrosses were cultured in vitro for several days and subsequently genotyped by PCR. Embryo outgrowths are composed of ICM surrounded by a single layer of TG cells.

In addition, BrdU labeling demonstrated that Emi1-deficient trophoblast cells remained alive and underwent DNA replication, even at the point when highly mitotic ICM cells apoptose (data not shown). Cells derived from ICM become highly proliferative, whereas TG cells are mitotically inactive at approximately E4.5 and undergo repeated rounds of S phase, generating a polyploid nucleus and large cytoplasm. These results indicate that Emi1 is not required for survival and proliferation of mitotic inactive TG cells, but it is essential for the continuity of highly proliferative ICM.

S phase of Emi1$^{-/-}$ embryonic cells. Based on our observation of preimplantation developmental failure, we postulate that Emi1-deficient embryos are defective in cell division or cycle progression from G_1 phase. Since human Emi1 promotes cyclin A accumulation and S-phase entry in somatic cells, we initially employed the in vitro cultures of pronuclei to ascertain whether the developmental failure of Emi1-deficient embryos resulted from cell proliferation defects. In an initial set of experiments, pronuclei cultured in vitro were pulse labeled for 10 min with BrdU, and BrdU-positive cells were quantitated by indirect immunofluorescence (Fig. 3). As shown in Fig. 3B, we detected 50 ± 5.5% BrdU-positive cells in Emi1-null embryos on average, compared to 45 ± 7.1% in control littermates, signifying no obvious defects in S-phase entry or progression in the former group. Thus, other abnormalities in Emi1-null embryos are prevalent in addition to cell proliferation defects.

Mitotic progression defects in Emi1-deficient embryos. Given that Emi1 inhibits APC activities at the S phase and early mitosis and degrades after mitosis entry, we initially assessed whether Emi1-null embryos display defects in mitotic entry by measuring the mitotic index of embryonic cells by immunostaining of phosphohistone H3 (Ser-10), a common mitotic marker that is specific for M-phase cells (11). Mitotic indexes were approximately 7.2 ± 0.5% and 9.0 ± 0.7% in both Emi1 WT and null embryonic cells, indicating no apparent defects in mitotic entry in the mutants. Moreover, most Emi1-null embryos underwent mitotic entry after nocodazole treatment (see Fig. S1 in the supplemental material). In vitro cultures of embryos and indirect immunofluorescence experiments were employed to ascertain whether Emi1-null embryonic cells display any defects in mitosis progression. Mitotic progression of embryonic cells was visualized by staining with alpha-tubulin and phosphohistone H3 (Ser-10).

Cells undergoing abnormal mitosis were frequently observed in Emi1-deficient embryos, but rarely in WT and heterozygous embryos. Under normal mitotic conditions, cells contain condensed chromosomes and a bipolar spindle (Fig. 4A, panels a, b, and c). Mitotic cells in prophase/prometaphase, metaphase, anaphase/telophase, and cytokinesis (Fig. 4A, panels d, e, f, and g, respectively) were observed in both WT and heterozygous embryos. In contrast, Emi1-null embryos contained cells undergoing mitotic catastrophe. Some cells exhibited overcondensed chromosomes and abnormal spindle structures at the

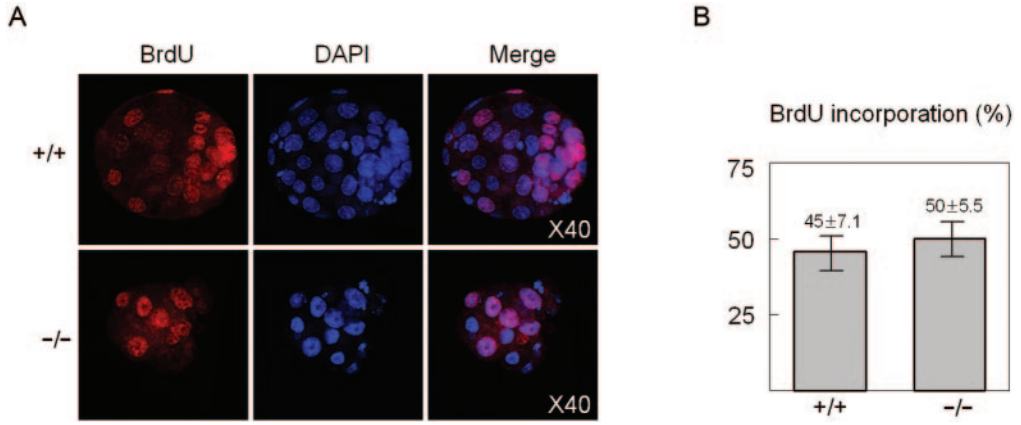

FIG. 3. S-phase progression in Emi1-deficient embryos. (A) S-phase progression was gauged by determining BrdU incorporation into in vitro-cultured pronuclei recovered from Emi1$^{+/-}$ intercrosses. Embryos were cultured in vitro for 96 h, pulsed for 10 min with BrdU, and processed for BrdU immunostaining and DAPI counterstaining. Magnification, ×40. (B) Series of *z*-plane images were stacked and analyzed by confocal microscopy (Zeiss) to precisely quantify the percentage of BrdU-positive cells in WT and Emi1$^{-/-}$ embryos. Error bars indicate standard deviations.

prometaphase-like stage (Fig. 4B, panels d and e), while others had misaligned chromosomes (Fig. 4B, panels f and g) or were in anaphase with multipolar and tangled spindle structures (Fig. 4B, panel g). Notably, multipolar spindles were additionally observed in nondestructive Emi1-expressing cells (18). The presence of these anaphase-like cells (Fig. 4B, panel g) signifies that Emi1-null cells prematurely undergo anaphase. Abnormal mitotic cells were observed in Emi1-null blastocysts at a high frequency (41 ± 8.4%) but were rarely observed in WT and heterozygous cells (Fig. 4C). These results collectively suggest that Emi1 is required for mitotic progression with fidelity.

Cell death in Emi1-null embryos. Most Emi1-deficient embryos developed into abnormal blastocysts, and many of the cells underwent mitotic catastrophe. In view of these findings, we propose that the defects in mitosis progress in Emi1-null cells result in increasing cell death in mutant conceptuses and, eventually, the destruction of the entire embryo. Consistent with this theory, DAPI staining revealed the presence of numerous condensed and fragmented nuclei, a hallmark of apoptotic cells, in Emi1-null embryos cultured in vitro (Fig. 4D). This result was further confirmed with the cell death detection assay. Following in vitro culture and terminal deoxynucleotidyltransferase-mediated dUTP-biotin nick end labeling (TUNEL) staining, TUNEL-positive cells were detected readily in Emi1$^{-/-}$ embryos, but rarely in heterozygous or WT littermates (Fig. 4D). Our data collectively suggest that cell death is responsible, at least in part, for the destruction of Emi1-null embryos.

Reduced level of cyclin A in Emi1-deficient embryos. Given that Emi1 inhibits APC activity in prophase, it is likely that its deficiency results in premature activation of the complex, thus prematurely triggering progression into anaphase. However, there are not many cells in early embryo with asynchronous stages; thus, it is technically difficult to directly test whether APC is prematurely activated in Emi1-deficient cells. As cyclin A degradation is inhibited by Emi1 at the S phase and prophase and follows Emi1 degradation at early mitosis, Emi1 deficiency may trigger partial or complete degradation of cyclin A. We performed indirect immunofluorescence experiments for APC substrates, especially cyclin A. Blastocysts recovered at E3.5 from heterozygote intercrosses were fixed and processed for cyclin A and cyclin D1 immunostaining. While cyclin D1 levels were similar in both WT cells and Emi1-deficient cells, relatively small amounts of cyclin A were detected in Emi1-deficient cells (Fig. 5) compared to those in WT cells. Considering that the only function of Emi1 is APC inhibition in S phase and prophase, these results may represent indirect evidence that APC is precociously activated in Emi1-deficient embryonic cells.

DISCUSSION

In this study, we performed genetic analysis of Emi1, an early mitotic inhibitor, in mice to evaluate its function in cell cycle progression. This protein is a key regulator of both G_1/S transition and mitotic progression, via its ability to inhibit the ubiquitin ligase activity of APC (12, 27, 28). Our analyses of Emi1-deficient embryos disclosed a critical and nonredundant function during murine preimplantation development. This conclusion is supported by the following observations: (i) *emi1* is expressed in oocytes during maturation (29) in embryos and in extraembryonic tissues during early embryogenesis (see Fig. S2 in the supplemental material), (ii) no Emi1$^{-/-}$ mice were detected among the 185 live births of Emi1$^{+/-}$ intercrosses, (iii) approximately 20% of embryos between E6.5 and E7.5 were fully resorbed, and (iv) Emi1$^{-/-}$ pronuclei recovered at swollen ampullae of oviducts of heterozygote intercrosses were detected at the expected Mendelian ratio (Table 1). Furthermore, upon recovery of pronuclei from heterozygote intercrosses cultured in vitro, we observed that Emi1$^{-/-}$ embryos were defective in preimplantation development, possibly due to mitotic abnormalities (Fig. 2D and 4B).

S-phase progression of Emi1$^{-/-}$ embryos is rarely defective, as evident from BrdU incorporation experiments (Fig. 3) and growth of blastocysts (Fig. 2E). In previous studies, the depletion of human Emi1 by RNA interference inhibited S-phase entry in somatic cells (12). Normal BrdU incorporation in Emi1-null embryos in this study may be explained by two

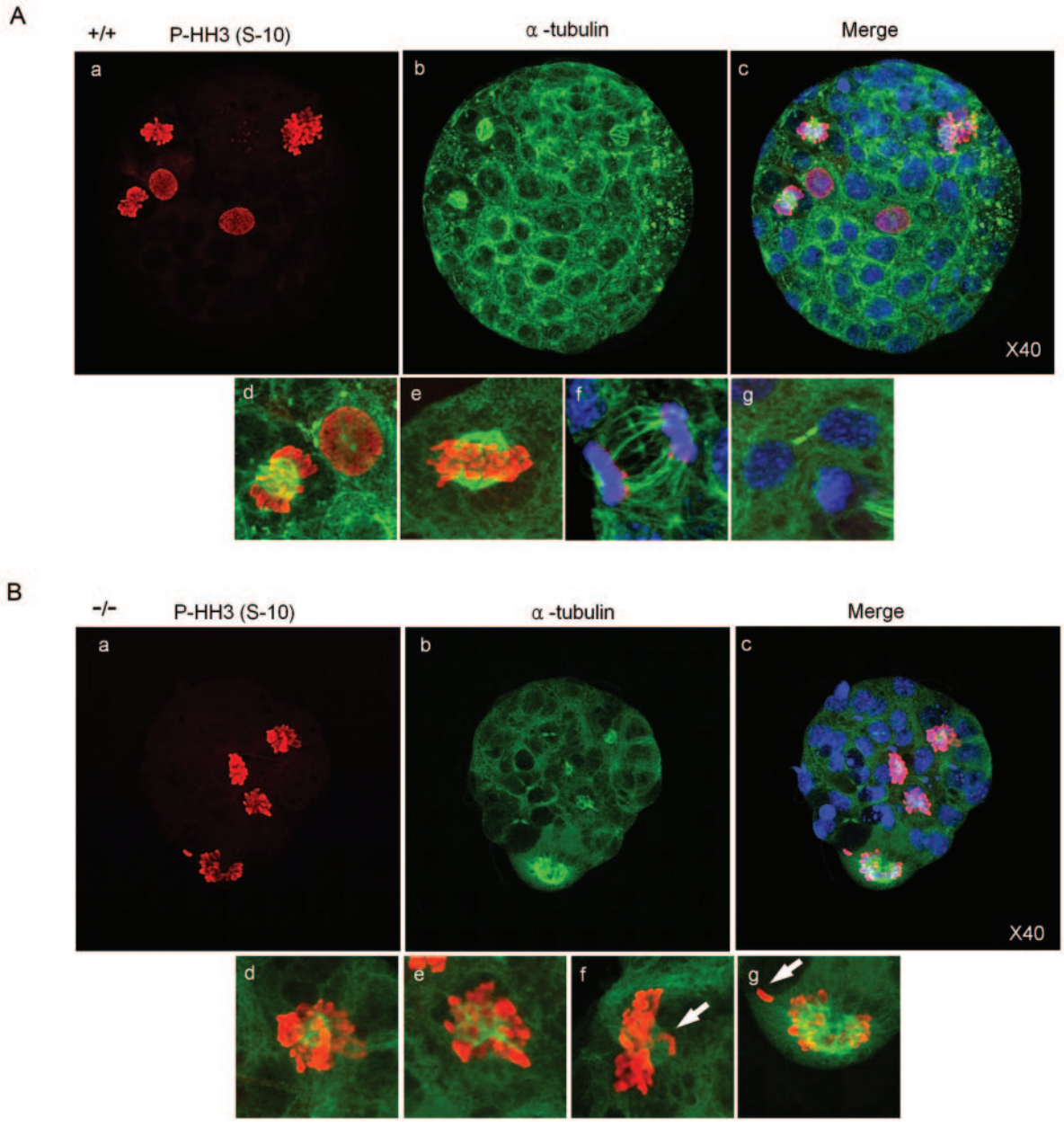
A
+/+
P-HH3 (S-10)
α -tubulin
Merge
a
b
c
X40
d
e
f
g
B
-/-
P-HH3 (S-10)
α -tubulin
Merge
a
b
c
X40
d
e
f
g
C
Abnormal mitosis (%)
41±8.4
40
20
2.5±0.3
+/+
-/-
D
+/+
-/-
X40
X40

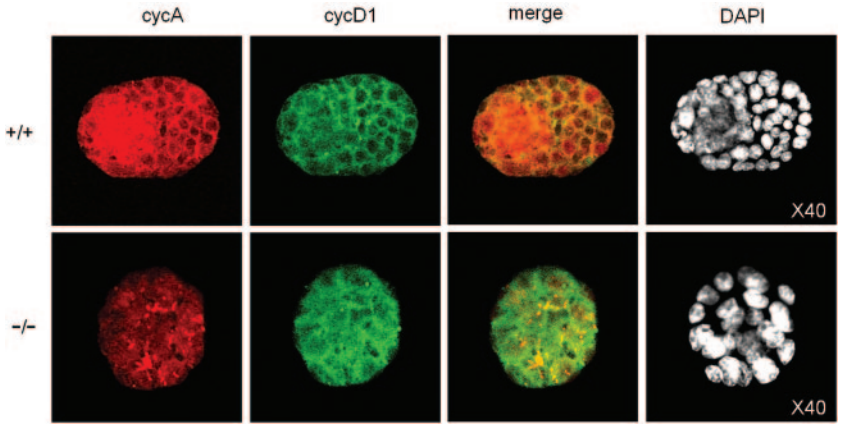

FIG. 5. The level of cyclin A was low in Emi1-deficient embryonic cells. Blastocysts recoverd at E3.5 from heterozygote intercrosses were fixed and processed for cyclin A (cycA) and cyclin D1 (cycD1) immunostaining as described in Materials and Methods. To measure the relative amounts of cyclin A and D1, embryonic cells were stained with anti-cyclin A antibodies (red), anti-cyclin D1 antibodies (green), and DAPI (white). After performing confocal microscopy (Zeiss), each embryo was genotyped. Magnification, ×40.

hypotheses. Since S-phase and mitosis succeed each other repeatedly with no intervening periods of cell growth during embryonic cycles, Emi1 may be dispensable for S-phase entry or progression of embryonic cells. Another possibility is that residual maternal Emi1 sufficiently compensates for loss of the zygotic protein.

Even though only 4% of cultured blatocysts were Emi1$^{-/-}$ in blastocyst outgrowth experiments, apoptosis of Emi1$^{-/-}$ cells is restricted to the rapidly dividing cells of the inner mass. Interestingly, the postmitotic polyploid trophoblast giant cells survive, suggesting that Emi1 is selectively required in mitosis. Abnormalities are additionally observed in approximately 40% of mitotic Emi1$^{-/-}$ cells compared to those in the WT. Mitotic Emi1$^{-/-}$ cells have multipolar spindles and misaligned chromosomes, which are rarely present in WT. Moreover, multipolar spindles are frequently observed in nondestructible Emi1-expressing cells (18).

The cell numbers of Emi1-null embryos during preimplantation development were always lower than those of the WT littermates (Fig. 4). This finding implies that embryos accumulate an abundance of mitotic errors, inevitably resulting in the cessation of development. Consistent with the above data, TUNEL-positive cells were detected readily in Emi1$^{-/-}$ embryos but rarely in heterozygous or WT littermates (Fig. 4D). Alteration of hEmi1 may affect the level and timing of APC activity, leading to genomic instability via several mechanisms (12, 18, 20, 25, 27, 28). Given the functional importance of Emi1 at the late prophase checkpoint, early embryonic death of Emi1$^{-/-}$ mice is possibly due to severe chromosomal instability. As cyclin B1-cdk1 is first activated in the centrosome in which Emi1 is localized (12, 13, 27), the absence of the protein may prematurely activate APC at centrosomes, thereby leading to premature anaphase transition and frequent chromosome misalignment/missegregation. The possibility of premature APC activation in Emi1-null cells was shown, even if indirectly, by immunostaining experiments in which the level of cyclin A, an APC substrate, was lower than that of cyclin D1 in the cells (Fig. 5). However, we cannot rule out the possibility that these defects in mitotic progression in Emi1-null cells are caused by another (unknown) function of the Emi1 protein. Due to the limitation of performing the experiments with embryonic cells and the early lethality of Emi1-deficient embryos, further experiments with cells in which *emi1* is conditionally removed are necessary to clarify the presence of premature APC activation in Emi1-deficient cells.

Chromosome misalignment/missegregation caused by Emi1 deficiency is a condition that daughter cells would not tolerate. Developmentally, most cell types are programmed not to allow aneuploidy formation in vivo and would conceivably be eliminated through apoptosis. Thus, it is not surprising that apoptotic cells are abundant in Emi1-deficient embryos (Fig. 4D).

An Emi1 homolog, Emi2/XErp1/FBXO43, which is conserved in amphibian, mouse, and human, has recently been reported as a novel Plx1-regulated inhibitor of APC activity during CSF arrest. However, how Emi2 inhibits APC ligase activity during the cell cycle and whether the two homologs have functional redundancies remain to be demonstrated. Our observations of the embryonic lethality of the Emi1$^{-/-}$ mouse

FIG. 4. Emi1$^{-/-}$ embryos exhibit M-phase progression defects and increased cell death. M-phase progression was explored by visualizing tubulin structure and histone H3 phosphorylation. Pronuclei were recovered from heterozygote intercrosses culture in vitro for 96 h, fixed, and processed for alpha-tubulin and phosphohistone H3 [P-HH3 (S-10)] immunostaining. Chromosomes were visualized by DAPI staining. After confocal microscopy (Zeiss), each embryo was genotyped. (A) WT embryos. (B) Emi1-deficient embryos. Each mitotic cell is magnified in panels d, e, f, and g. Arrows indicate misaligned chromosomes. (C) Series of *z*-plane images were stacked and analyzed by confocal microscopy to precisely quantify the percentage of abnormal mitotic cells in WT and Emi1$^{-/-}$ embryos. Error bars indicate standard deviations. (D) Increased apoptosis in Emi1-deficient embryos. DNA fragmentation associated with apoptosis was detected with an in situ cell death detection kit (Chemicon), following the manufacturer's instructions. Merged images were obtained from representative WT and Emi1$^{-/-}$ pronuclei cultured for 72 h and processed for DAPI and TUNEL staining. Magnification, ×40.

indicate that Emi1 is not functionally redundant with and compensated by Emi2.

Notably, mice from several strains engineered to lack proteins involved in the spindle assembly checkpoint that inhibits APC activity in metaphase die at the peri-implantation stage, with mitotic abnormalities resembling those identified in Emi1-deficient embryos. These strains include Mad2 (4), survivin (35), Bub3 (14), BubR1 (37), Incenp (3), and CENP-E (26) mutants. Genetic data suggest that the late prophase checkpoint by Emi1 is as important as the spindle assembly checkpoint in mitotic progression and chromosome stability. However, unlike Mad- and BubR1-heterozygous mice, Emi1-heterozygous mice display no developmental abnormalities until 18 months, indicating that one functional copy of the Emil gene is sufficient for normal growth.

However, mice lacking Rassf1A, another regulator of APC activity in early mitosis, show no defects in murine embryo development but only tumor susceptibility (33, 36). These Rassf1A genetic data may suggest that the inhibitory functions of the gene product are restricted in unusual or stress conditions, although the proteins potentially display APC regulation. Alternatively, it is possible that other members of the RASSF1 family functionally compensate for the loss of Rassf1A in mice.

Our analyses in mice clearly imply that the Emi1 protein is required for mitotic fidelity. The Emi1 mutation in mice was difficult to study due to the severity of the phenotypes. Thus, tissue-specific or conditional knockout experiments in mice are required for further clarification of Emi1 function.

ACKNOWLEDGMENTS

We are grateful to Phillip Soriano and Allan Bradley for the mouse embryonic stem cells AK7 and SNL6 feeder, respectively.

This study was supported by the National Research Laboratory Program, the Korea National Cancer Center Control Program (0320370-1 and 0510582-2), and the 21st Century Frontier Functional Human Genome Project of KISTEP (Ministry of Science and Technology of Korea).

REFERENCES

1. **Ang, X. L., and J. Wade Harper.** 2005. SCF-mediated protein degradation and cell cycle control. Oncogene **24:**2860–2870.
2. **Castro, A., C. Bernis, S. Vigneron, J. C. Labbe, and T. Lorca.** 2005. The anaphase-promoting complex: a key factor in the regulation of cell cycle. Oncogene **24:**314–325.
3. **Cutts, S. M., K. J. Fowler, B. T. Kile, L. L. Hii, R. A. O'Dowd, D. F. Hudson, R. Saffery, P. Kalitsis, E. Earle, and K. H. Choo.** 1999. Defective chromosome segregation, microtubule bundling and nuclear bridging in inner centromere protein gene (*Incenp*)-disrupted mice. Hum. Mol. Genet. **8:**1145–1155.
4. **Dobles, M., V. Liberal, M. L. Scott, R. Benezra, and P. K. Sorger.** 2000. Chromosome missegregation and apoptosis in mice lacking the mitotic checkpoint protein Mad2. Cell **101:**635–645.
5. **Dong, X., K. H. Zavitz, B. J. Thomas, M. Lin, S. Campbell, and S. L. Zipursky.** 1997. Control of G_1 in the developing Drosophila eye: rca1 regulates cyclin A. Genes Dev. **11:**94–105.
6. **Fuchs, S. Y., V. S. Spiegelman, and K. G. Kumar.** 2004. The many faces of beta-TrCP E3 ubiquitin ligases: reflections in the magic mirror of cancer. Oncogene **23:**2028–2036.
7. **Guardavaccaro, D., Y. Kudo, J. Boulaire, M. Barchi, L. Busino, M. Donzelli, F. Margottin-Goguet, P. K. Jackson, L. Yamasaki, and M. Pagano.** 2003. Control of meiotic and mitotic progression by the F box protein beta-Trcp1 in vivo. Dev. Cell **4:**799–812.
8. **Hansen, D. V., A. V. Loktev, K. H. Ban, and P. K. Jackson.** 2004. Plk1 regulates activation of the anaphase promoting complex by phosphorylating and triggering $SCF^{\beta TrCP}$-dependent destruction of the APC inhibitor Emi1. Mol. Biol. Cell **15:**5623–5634.
9. **Harper, J. W., J. L. Burton, and M. J. Solomon.** 2002. The anaphase-promoting complex: it's not just for mitosis any more. Genes Dev. **16:**2179–2206.
10. **Hart, M., J. P. Concordet, I. Lassot, I. Albert, R. del los Santos, H. Durand, C. Perret, B. Rubinfeld, F. Margottin, R. Benarous, and P. Polakis.** 1999. The F-box protein beta-TrCP associates with phosphorylated beta-catenin and regulates its activity in the cell. Curr. Biol. **9:**207–210.
11. **Hendzel, M. J., Y. Wei, M. A. Mancini, A. Van Hooser, T. Ranalli, B. R. Brinkley, D. P. Bazett-Jones, and C. D. Allis.** 1997. Mitosis-specific phosphorylation of histone H3 initiates primarily within pericentromeric heterochromatin during G_2 and spreads in an ordered fashion coincident with mitotic chromosome condensation. Chromosoma **106:**348–360.
12. **Hsu, J. Y., J. D. Reimann, C. S. Sorensen, J. Lukas, and P. K. Jackson.** 2002. E2F-dependent accumulation of hEmi1 regulates S phase entry by inhibiting APC^{Cdh1}. Nat. Cell Biol. **4:**358–366.
13. **Jackman, M., C. Lindon, E. A. Nigg, and J. Pines.** 2003. Active cyclin B1-Cdk1 first appears on centrosomes in prophase. Nat. Cell Biol. **5:**143–148.
14. **Kalitsis, P., E. Earle, K. J. Fowler, and K. H. Choo.** 2000. Bub3 gene disruption in mice reveals essential mitotic spindle checkpoint function during early embryogenesis. Genes Dev. **14:**2277–2282.
15. **Le Cam, L., M. Lacroix, M. A. Ciemerych, C. Sardet, and P. Sicinski.** 2004. The E4F protein is required for mitotic progression during embryonic cell cycles. Mol. Cell. Biol. **24:**6467–6475.
16. **Lew, D. J., and D. J. Burke.** 2003. The spindle assembly and spindle position checkpoints. Annu. Rev. Genet. **37:**251–282.
17. **Lim, D. S., and P. Hasty.** 1996. A mutation in mouse rad51 results in an early embryonic lethal that is suppressed by a mutation in p53. Mol. Cell. Biol. **16:**7133–7143.
18. **Margottin-Goguet, F., J. Y. Hsu, A. Loktev, H. M. Hsieh, J. D. Reimann, and P. K. Jackson.** 2003. Prophase destruction of Emi1 by the $SCF^{betaTrCP/Slimb}$ ubiquitin ligase activates the anaphase promoting complex to allow progression beyond prometaphase. Dev. Cell **4:**813–826.
19. **Michel, L. S., V. Liberal, A. Chatterjee, R. Kirchwegger, B. Pasche, W. Gerald, M. Dobles, P. K. Sorger, V. V. Murty, and R. Benezra.** 2001. MAD2 haplo-insufficiency causes premature anaphase and chromosome instability in mammalian cells. Nature **409:**355–359.
20. **Moshe, Y., J. Boulaire, M. Pagano, and A. Hershko.** 2004. Role of Polo-like kinase in the degradation of early mitotic inhibitor 1, a regulator of the anaphase promoting complex/cyclosome. Proc. Natl. Acad. Sci. USA **101:**7937–7942.
21. **Murray, A. W., M. J. Solomon, and M. W. Kirschner.** 1989. The role of cyclin synthesis and degradation in the control of maturation promoting factor activity. Nature **339:**280–286.
22. **Musacchio, A., and K. G. Hardwick.** 2002. The spindle checkpoint: structural insights into dynamic signalling. Nat. Rev. Mol. Cell Biol. **3:**731–741.
23. **Nagy, A., M. Gertsenstein, K. Vintersten, and R. Behringer.** 2003. Manipulating the mouse embryo: a laboratory manual, 3rd ed. Cold Spring Harbor Laboratory Press, Cold Spring Harbor, N.Y.
24. **Peters, J. M.** 2002. The anaphase-promoting complex: proteolysis in mitosis and beyond. Mol. Cell **9:**931–943.
25. **Peters, J. M.** 2003. Emi1 proteolysis: how $SCF^{\beta\text{-}Trcp1}$ helps to activate the anaphase-promoting complex. Mol. Cell **11:**1420–1421.
26. **Putkey, F. R., T. Cramer, M. K. Morphew, A. D. Silk, R. S. Johnson, J. R. McIntosh, and D. W. Cleveland.** 2002. Unstable kinetochore-microtubule capture and chromosomal instability following deletion of CENP-E. Dev. Cell **3:**351–365.
27. **Reimann, J. D., E. Freed, J. Y. Hsu, E. R. Kramer, J. M. Peters, and P. K. Jackson.** 2001. Emi1 is a mitotic regulator that interacts with Cdc20 and inhibits the anaphase promoting complex. Cell **105:**645–655.
28. **Reimann, J. D., B. E. Gardner, F. Margottin-Goguet, and P. K. Jackson.** 2001. Emi1 regulates the anaphase-promoting complex by a different mechanism than Mad2 proteins. Genes Dev. **15:**3278–3285.
29. **Reimann, J. D., and P. K. Jackson.** 2002. Emi1 is required for cytostatic factor arrest in vertebrate eggs. Nature **416:**850–854.
30. **Schmidt, A., P. I. Duncan, N. R. Rauh, G. Sauer, A. M. Fry, E. A. Nigg, and T. U. Mayer.** 2005. *Xenopus* polo-like kinase Plx1 regulates XErp1, a novel inhibitor of APC/C activity. Genes Dev. **19:**502–513.
31. **Song, M. S., and D. S. Lim.** 2004. Control of APC-Cdc20 by the tumor suppressor RASSF1A. Cell Cycle **3:**574–576.
32. **Song, M. S., S. J. Song, N. G. Ayad, J. S. Chang, J. H. Lee, H. K. Hong, H. Lee, N. Choi, J. Kim, H. Kim, J. W. Kim, E. J. Choi, M. W. Kirschner, and D. S. Lim.** 2004. The tumour suppressor RASSF1A regulates mitosis by inhibiting the APC-Cdc20 complex. Nat. Cell Biol. **6:**129–137.
33. **Tommasi, S., R. Dammann, Z. Zhang, Y. Wang, L. Liu, W. M. Tsark, S. P. Wilczynski, J. Li, M. You, and G. P. Pfeifer.** 2005. Tumor susceptibility of Rassf1a knockout mice. Cancer Res. **65:**92–98.
34. **Tung, J. J., D. V. Hansen, K. H. Ban, A. V. Loktev, M. K. Summers, J. R. Adler III, and P. K. Jackson.** 2005. A role for the anaphase-promoting complex inhibitor Emi2/XErp1, a homolog of early mitotic inhibitor 1, in

cytostatic factor arrest of *Xenopus* eggs. Proc. Natl. Acad. Sci. USA **102:** 4318–4323.

35. **Uren, A. G., L. Wong, M. Pakusch, K. J. Fowler, F. J. Burrows, D. L. Vaux, and K. H. Choo.** 2000. Survivin and the inner centromere protein INCENP show similar cell-cycle localization and gene knockout phenotype. Curr. Biol. **10:**1319–1328.
36. **van der Weyden, L., K. K. Tachibana, M. A. Gonzalez, D. J. Adams, B. L. Ng, R. Petty, A. R. Venkitaraman, M. J. Arends, and A. Bradley.** 2005. The RASSF1A isoform of RASSF1 promotes microtubule stability and suppresses tumorigenesis. Mol. Cell. Biol. **25:**8356–8367.
37. **Wang, Q., T. Liu, Y. Fang, S. Xie, X. Huang, R. Mahmood, G. Ramaswamy, K. M. Sakamoto, Z. Darzynkiewicz, M. Xu, and W. Dai.** 2004. BUBR1 deficiency results in abnormal megakaryopoiesis. Blood **103:**1278–1285.
38. **Winston, J. T., P. Strack, P. Beer-Romero, C. Y. Chu, S. J. Elledge, and J. W. Harper.** 1999. The $SCF^{\beta\text{-}TRCP}$-ubiquitin ligase complex associates specifically with phosphorylated destruction motifs in IκBα and β-catenin and stimulates IκBα ubiquitination in vitro. Genes Dev. **13:**270–283.
39. **Yan, L., and R. Silver.** 2002. Differential induction and localization of mPer1 and mPer2 during advancing and delaying phase shifts. Eur. J. Neurosci. **16:**1531–1540.
40. **Yu, H.** 2002. Regulation of APC-Cdc20 by the spindle checkpoint. Curr. Opin. Cell Biol. **14:**706–714.